Pacemaker-driven stochastic resonance on diffusive and complex networks of bistable oscillators

2008 New J. Phys. 10 053008

(http://iopscience.iop.org/1367-2630/10/5/053008)

New Journal of Physics
The open–access journal for physics

Pacemaker-driven stochastic resonance on diffusive and complex networks of bistable oscillators

Matjaž Perc[1] **and Marko Gosak**

Department of Physics, Faculty of Natural Sciences and Mathematics, University of Maribor, Koroška cesta 160, SI-2000 Maribor, Slovenia
E-mail: matjaz.perc@uni-mb.si

New Journal of Physics **10** (2008) 053008 (21pp)
Received 5 December 2007
Published 7 May 2008
Online at http://www.njp.org/
doi:10.1088/1367-2630/10/5/053008

Abstract. We study the phenomenon of stochastic resonance on diffusive, small-world and scale-free networks consisting of bistable overdamped oscillators. Important thereby is the fact that the external subthreshold periodic forcing is introduced only to a single oscillator of the network. Hence, the forcing acts as a pacemaker trying to impose its rhythm on the whole network through the unit to which it is introduced. Without the addition of additive spatiotemporal noise, however, the whole network, including the unit that is directly exposed to the pacemaker, remains trapped forever in one of the two stable steady states of the local dynamics. We show that the correlation between the frequency of subthreshold pacemaker activity and the response of the network is resonantly dependent on the intensity of additive noise. The reported pacemaker-driven stochastic resonance depends most significantly on the coupling strength and the underlying network structure. Namely, the outreach of the pacemaker obeys the classic diffusion law in the case of nearest-neighbor interactions, thus being proportional to the square root of the coupling strength, whereas it becomes superdiffusive by an appropriate small-world or scale-free topology of the interaction network. In particular, the scale-free topology is identified as being optimal for the dissemination of localized rhythmic activity across the whole network. Also, we show that the ratio between the clustering coefficient and the characteristic path length is the crucial quantity defining the ability of a small-world network to facilitate the outreach of the pacemaker-emitted subthreshold rhythm. We additionally confirm these findings by using the FitzHugh–Nagumo excitable system as an alternative to the bistable overdamped oscillator.

[1] Author to whom any correspondence should be addressed.

Contents

1. Introduction

The study of noise-induced constructive effects in nonlinear dynamical systems has gained a lot of attention in the last two decades [1]. Two of the perhaps most famous phenomena are stochastic resonance (examples of reviews are [2]), where noise enhances the response of a system to weak external forcing in a resonant manner, and coherence resonance [3], where the impact of noise alone induces coherent system behavior. Seminal works within the context of stochastic resonance have been related to the analysis of the response of a stochastic overdamped bistable system [4]. Later on, the mechanism of stochastic resonance was reported in excitable systems [5], whereby excitability has subsequently been noted as an important system property for a broad variety of noise-induced phenomena [6]. In contrast to bistable systems, excitable systems have one stable steady state, but possess a threshold to an unstable excited state that manifests as a large amplitude deviation from the stable steady state. In addition, proximities to special bifurcation points have also received substantial attention as being possible mechanisms for stochastic and coherence resonance [7]. Notably, stochastic and coherence resonance have also been reported in systems exhibiting bimodal chaos [8].

Following initial advances in understanding effects of noise on individual dynamical systems, the scope shifted to spatially extended systems. Primary investigations were focused on the stochastic resonance in coupled nonlinear overdamped oscillators [9]. Later on, similar systems served for several other reports about non-trivial effects of noise, such as array-enhanced stochastic resonance [10], diversity-induced resonance [11] and system size resonance [12]. Of course, spatio-temporal stochastic and coherence resonance were also reported in other set-ups, for instance in excitable media [13], but since investigations in this direction grow so fast, it is impossible to overview here all the relevant contributions. Therefore, reference [14] should only be considered as a guide for interested readers.

While in the past the majority of scientific research dealing with the dynamics of spatially extended systems was devoted to the study of regular diffusively coupled networks, recently, the focus has been shifting toward networks with more complex topologies [15]. Since already a small fraction of random links between distant units largely decreases the typical path length between two arbitrary sites, such networks were termed appropriately as ‘small-world’ networks [16]. On the other hand, growth and preferential attachment may result in networks with a power-law degree distribution, hence the name ‘scale-free’ networks fits best [17]. Importantly, networks with small-world or scale-free properties appear to be excellent

for modeling interactions among units of complex systems. Examples range from social networks [18], scientific-collaboration networks [19], food webs [20], computer networks [21], as well as neural and excitable networks in general [22].

Stochastic resonance has already been studied in networks with small-world topology. Particularly, it has been shown that the output of a network of coupled bistable overdamped oscillators can be further improved by increasing the number of random shortcut links, whereby the ordering effect depends largely on the coupling strength and the fraction of rewired links [23]. Subsequently, the idea has also been applied to opinion formation models [24], where the role of randomness and connectivity, combined with external periodic modulation representing a so-called 'fashion wave' has been studied. Recently, an interesting study about the amplification of signals in scale-free networks of bistable oscillators has also been published [25]. Moreover, the coherence resonance has been reported on small-world networks [26], as was pattern formation in two-dimensional, small-world media [27], and the ability of complex topologies to suppress spatiotemporal chaotic behavior [28].

Presently, we wish to expand the scope of stochastic resonance on diffusive small-world and scale-free networks by studying its emergence in the presence of subthreshold pacemaker activity. Pacemakers are isolated units in the system that dictate the operating rhythm of neighboring units, i.e. pace, and so guide the functioning of a larger ensemble. Due to the considerable importance of pacemakers in real-life systems, some studies have already been devoted to their impact on excitable systems [29], as well as on networks with small-world topology [30]. To extend the subject, we study the possibility of stochastic resonance on a network of overdamped bistable oscillators via a pacemaker. More precisely, we introduce a subthreshold periodic pacemaker to one unit of the network and study the noise-supported outreach of the pacemaker to other units of the network. We show that the correlation between the periodic driving and the response of the system depends resonantly on the noise intensity. Moreover, for diffusive nearest-neighbor interactions there is a square root relationship between the outreach of the pacemaker and the coupling constant, thus indicating the applicability of the classical diffusion law. However, in the case of small-world connectivity the latter relationship becomes superdiffusive provided the topology is adequately adjusted. Namely, we demonstrate that there exists an optimal fraction of rewired links, determined by the clustering coefficient and the characteristic path length of the underlying small-world network, at which the noise-induced spreading of pacemaker activity is pronounced best. We support the latter finding further by considering as an alternative model to the bistable oscillator the FitzHugh–Nagumo excitable system [31], showing that such qualitative differences in the dynamics do not affect the properties of optimal small-world topology. Finally, we also consider the scale-free interaction topology amongst bistable oscillators, whereby the pacemaker is introduced to the main hub of the network. We find that the scale-free topology warrants the best noise-supported dissemination of pacemaker-emitted rhythmic activity across the whole network, albeit at the expense of a lower correlation with the directly paced unit when compared to the diffusive case. Again, this result is shown to be independent of differences between the bistable and the FitzHugh–Nagumo excitable dynamics governing the network.

The paper is structured as follows. In section 2, we introduce the bistable overdamped oscillator and the FitzHugh–Nagumo model, as well as considered networks and other mathematical methods presently in use. Results are presented in sections 3, 4 and 5 separately for diffusive, small-world and scale-free networks, respectively. In the last section, we summarize the results and briefly comment on the potential applicability of our findings.

2. Mathematical models and set-up

The main model to be used presently consists of noisy bistable overdamped oscillators, governed by the Langevin equations of the form

$$\frac{\mathrm{d}x_i}{\mathrm{d}t} = x_i - x_i^3 + \sum_j \varepsilon_{ij}(x_j - x_i) + \sqrt{2D}\xi_i(t), \tag{1}$$

where ε_{ij} is the coupling strength between units i and j, while $2D$ is the variance of Gaussian noise with zero mean and autocorrelation $\langle \xi_i(t)\xi_j(t')\rangle = \delta_{ij}\delta(t-t')$. In the thermodynamic limit, the model given by equation (1) exhibits an Ising-type phase transition by a critical coupling strength [32], taking it from the disordered phase, characterized by a vanishing mean field, to an ordered phase with a finite mean field, corresponding to one of the two symmetric stable steady states of the local dynamics centered around ± 1 that correspond to the minima of the pertaining potential energy function $V(x_i) = -\mathrm{x}_i^2/2 + x_i^4/4$. For finite system sizes, on the other hand, the ordered phase is characterized by irregular switches between the two possible finite mean fields, whose average is again vanishing irrespective of the coupling strength. As already argued [12], in the bistable case equation (1) provides a paradigmatic set-up for stochastic resonance, hence implying that a fine tuning of D might optimize the response of the model to a subthreshold periodic forcing in a resonant manner.

To widen the scope of our findings, we occasionally consider as an alternative to the above bistable model, small-world as well as scale-free networks characterized with the FitzHugh–Nagumo excitable dynamics [31] of the form

$$\begin{aligned} \kappa\frac{\mathrm{d}u_i}{\mathrm{d}t} &= u_i(1-u_i)\left[u_i - \frac{(v_i+b)}{a}\right] + \sum_j \varepsilon_{ij}(u_j - u_i) + \sqrt{2D}\xi_i(t), \\ \frac{\mathrm{d}v_i}{\mathrm{d}t} &= u_i - v_i, \end{aligned} \tag{2}$$

where the Gaussian noise has exactly the same properties as in equation (1). Moreover, $\kappa = 0.02$ implies that the dynamics of u_i is much faster than that of v_i, thus providing the necessary ingredient for excitability. For parameter values $a = 0.75$ and $b = 0.01$ each FitzHugh–Nagumo unit is governed by a single stable excitable steady state $u_i = v_i = 0$. Weak perturbations of this state may give rise to large-amplitude excursions toward $u_i = v_i = 1$, which however, is unstable resulting in a quick reoccupation of $u_i = v_i = 0$. The excitable dynamics of the FitzHugh–Nagumo system is thus qualitatively different from the one characterizing the bistable oscillator. Nevertheless, both the bistable as well as the excitable dynamics (see review in [6]) have proven viable candidates for the observation of stochastic resonance, and it is interesting to examine whether differences between them result in qualitatively different behavior within this study.

To explore the possibility of stochastic resonance, we presently introduce a subthreshold pacemaker of the form $f_r(t) = A\cos(\omega t)$ to a single unit $i = r$ [variable $u_i = u_r$ by equation (2)] of the network, which remains exposed to the periodic forcing during the whole simulation period. Throughout this study, we use $A = 0.08$ and $\omega = \pi/300$ for the bistable oscillator and $A = 0.02$ and $\omega = 0.7$ for the FitzHugh–Nagumo model, which warrant that in the absence of noise ($D = 0$) the pacemaker is subthreshold, meaning it cannot by itself induce transitions between the two stable steady states or evoke large-amplitude excitations; not by the unit which is directly exposed and neither by any other constitutive unit of the network.

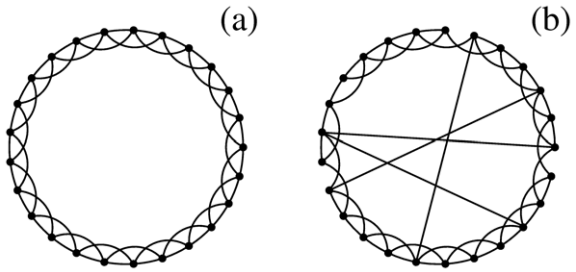

Figure 1. Examples of considered network topologies. For clarity regarding k and p only 25 vertices are displayed in each panel. (a) Regular ring characterized by $p = 0$ with periodic boundary conditions. Each vertex is connected to its $k = 4$ nearest neighbors. (b) Realization of small-world topology via random rewiring of a certain fraction p of links (in this case 4 out of all 100 were rewired, hence $p = 0.04$).

Instead, the unit directly perturbed by the pacemaker (as well as those directly linked to it, but to a much lesser extent depending on the coupling strength) exhibits small-amplitude oscillations around the stable steady state with the frequency ω.

As announced, we consider diffusive and small-world networks constituting the interactions amongst coupled units, which we obtain via the procedure described in [16] by starting from a regular ring with periodic boundary conditions, comprising $N = 200$ vertices each having connectivity $k = 4$, as shown in figure 1(a). In this scheme, each vertex (or unit) corresponds to one noise-driven overdamped bistable oscillator or one FitzHugh–Nagumo system (depending on which dynamics we use). The probability of rewiring a link is denoted by p and can occupy any value from the unit interval, whereby $p = 0$ constitutes a regular graph while $p = 1$ results in a random network. For $0 < p < 1$, as exemplified in figure 1(b), the resulting network may have small-world properties in that the normalized characteristic path length L between distant units is small, i.e. comparable with that of a random network, while the normalized clustering coefficient C is still large, i.e. comparable with that of a regular nearest-neighbor graph constituting diffusive interactions amongst coupled units. According to [16], the characteristic path length is defined as the average number of edges in the shortest path between any two vertices, while the clustering coefficient is the average fraction of all $k_i(k_i - 1)/2$ allowable edges that actually exist amongst vertex i and all its k_i neighbors. Furthermore, in section 5 we use scale-free networks generated via growth and preferential attachment as proposed by Barabási and Albert [17], again comprising $N = 200$ vertices and having average degree $k = 4$. Since the degree distribution of such networks is of power-law-type with the slope of the line equaling -2.9 on a double logarithmic graph, the degree inhomogeneity of individual vertices forming such a scale-free network is substantial. Here, we consider the introduction of the pacemaker to the vertex with the highest degree (main hub), as the latter seems optimally suited for disseminating weak localized rhythmic activity across the whole network. Note that by small-world networks the degree inhomogeneity follows a Poissonian distribution (in the limit $p \to 1$) centered around $k = 4$. Hence, small-world networks are statistically more homogeneous, and therefore the particular placing of the pacemaker within them is not so crucial. If by any of the employed networks vertices i and j are connected then $\varepsilon_{ij} = \varepsilon_{ji} = \varepsilon$ but otherwise $\varepsilon_{ij} = \varepsilon_{ji} = \varepsilon_{ii} = 0$ in equations (1) and (2).

For each set of the two main parameters ε and D, as well as the employed network topology, the temporal output of each unit is recorded for $T = 3000$ periods of the pacemaker, and the correlation of each series with the frequency of the pacemaker $\omega = 2\pi/t_f$ is computed via the Fourier coefficients $Q_i = \sqrt{R_i^2 + S_i^2}$ according to [33]:

$$R_i = \frac{2}{t_f T} \int_0^{t_f T} x_i \sin(\omega t)\, \mathrm{d}t, \qquad S_i = \frac{2}{t_f T} \int_0^{t_f T} x_i \cos(\omega t)\, \mathrm{d}t. \tag{3}$$

If the FitzHugh–Nagumo excitable system given by equation (2) is used for the description of network dynamics, then x_i in equation (3) is replaced by u_i. Since the Fourier coefficients are exactly proportional to the (square of the) spectral power amplification [34], which is frequently used as a measure for stochastic resonance, the signal-to-noise ratio (SNR) for each bistable oscillator is simply given by Q_i. Importantly, the final results presented in the figures later in the paper were obtained by averaging the SNR over up to 100 different realizations of network configurations and initial conditions for each set of parameters.

3. Diffusive networks

We start by examining the results obtained if the bistable oscillators are coupled exclusively in a diffusive manner, as exemplified in figure 1(a). Hence, throughout this section, we set $p = 0$. First, we consider space–time plots obtained by a given ε and different D. Panels in figure 2 feature the results. For small D (top two panels in figure 2), noise is clearly unable to induce frequent shifts between the two steady states as all coupled units exhibit lengthy and highly irregular stays in one of the two minima of the corresponding potential. Moreover, even the unit directly perturbed by the pacemaker ($i = r = 100$) and its immediate neighbors do not benefit from their special status, because noisy perturbations are too weak to assist the pacemaker strongly enough to evoke shifts between the two minima of the potential in accordance with the frequency of the subthreshold periodic driving. In sharp contrast, for large D (bottom two panels in figure 2) shifts between the two steady states are constant, but also irregular. In particular, also the units around the pacemaker oscillate much more frequently than would be necessary to warrant a good correlation with the subthreshold periodic driving. Finally, for an intermediate value of D (middle two panels in figure 2), the space–time plot is also quite far from being nicely correlated with the pacemaker, but nevertheless, the graining of the color map along the temporal direction does provide subtle clues that indeed the temporal output of the network might be better correlated with the localized periodic driving than by the former two cases. The validity of this conclusion is additionally amplified by the temporal output of the unit directly perturbed by the pacemaker and its nearest neighbors, where clearly the shifts between the two steady states often follow the pacemaker in a quite convincing manner. Although more persuasive pictures of temporal and/or spatial dynamics are usually shown as first evidence for stochastic resonance, we included these space–time plots to emphasize: firstly, that the outreach of the pacemaker seems to decay fast with the distance from the origin if diffusive coupling is employed and secondly, that the phenomenon is rather subtle and requires extensive computer simulations for proper and in-depth treatment. In what follows, we will support the existence of stochastic resonance more firmly via the SNR, and study the phenomenon in dependence on D and ε, as well as the distance from the unit directly perturbed by the pacemaker.

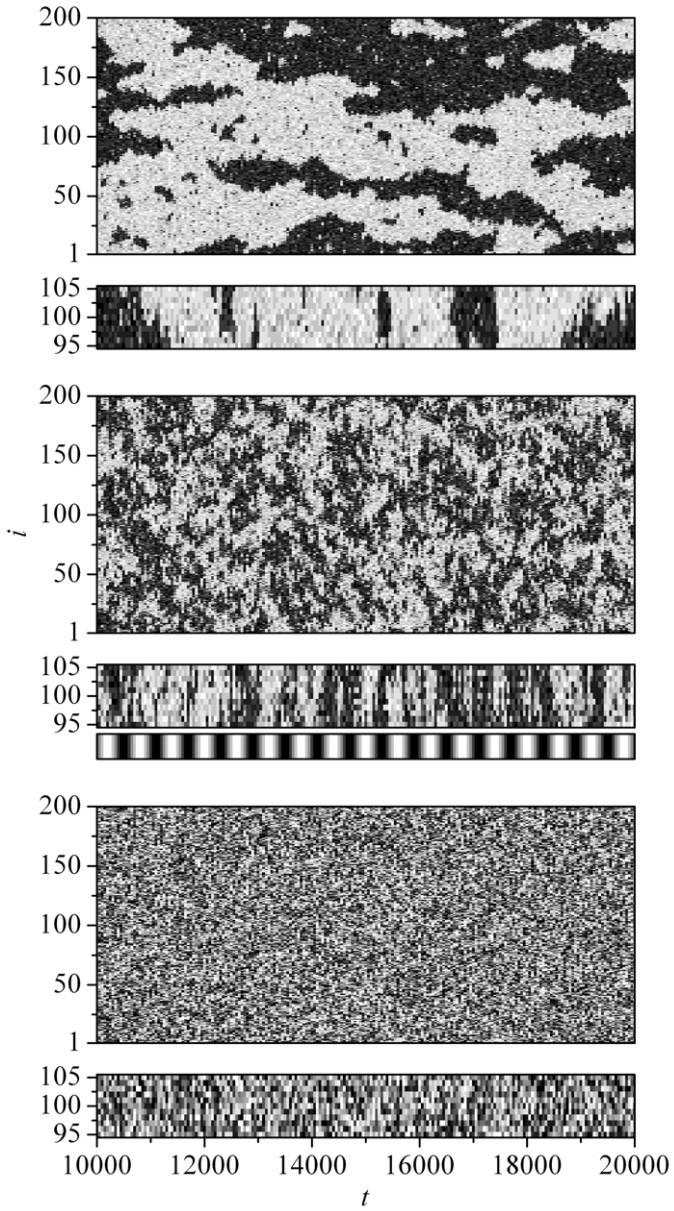

Figure 2. Space–time plots obtained with the bistable dynamics [equation (1)] by $p = 0$ and $\varepsilon = 0.0625$ for $D = 0.05$ (top two panels), $D = 0.12$ (middle two panels), and $D = 0.5$ (bottom two panels). By all three cases the pacemaker has been introduced to the middle oscillator $i = r = 100$, and the narrower space–time plots show an excerpt of the whole network around the pacemaker-driven unit. The color profile in all panels is linear, white depicting $x_i = -1.5$ and black $x_i = 1.5$. A color stripe indicating the frequency of the pacemaker is also shown for easier comparisons.

Figure 3 features color-contour plots of SNR in dependence on D and i (index for coupled units) for different ε. Presented results convey that there indeed exists a maximum of SNR for an intermediate value of D irrespective of ε, albeit the value of the coupling strength crucially determines to what extent this holds also for units that are not in the immediate proximity of the oscillator $i = r = 100$ that is under the direct influence of the pacemaker. More precisely, while the stochastic resonance is clearly inferable for nearby neighbors of the pacemaker-driven oscillator for all ε, more distinct units are able to correlate their noise-induced oscillations with the subthreshold driving only if ε is large. Results in figure 3 show that by diffusive networks coupling strengths as high as $\varepsilon = 2$ (or higher) may be necessary to warrant that *all* units comply (at least to some extent) with the frequency of the pacemaker by an intermediate D. Nevertheless, the presented color-contour plots provide ample evidence for pacemaker-driven stochastic resonance in a diffusively coupled network of bistable oscillators.

What figure 3 somewhat fails to convey accurately is that the price for an outreach of the pacemaker even to the most distinct units of the network is a rather steep drop of the overall maximal SNR, which sets in due to increasing values of ε required for transmitting the localized subthreshold stimulus across the whole diffusively coupled network. To elaborate on this fact, we present in figure 4(a) SNR curves in dependence on D only for the oscillator that is under the direct influence of the pacemaker. As is evident already from the results presented in figure 3, this is the unit of the network by which the most correlated response with respect to the subthreshold periodic driving sets in, and accordingly, the overall maximal SNR is obtained. Indeed, the left panel of figure 4 shows that the peak value of SNR drops by an order of magnitude as the coupling strength increases from $\varepsilon = 0.0625$ to 4.0. This is also in agreement with the fact that the optimal D increases continuously with increasing ε. Note that higher D directly contribute to a lower value of SNR, because the level of background noise is accordingly higher also in the system's output. To elucidate the subtleties of the examined stochastic resonance phenomenon further, the right panel of figure 4 shows SNR curves in dependence on i by the value of D warranting the peak SNR by a given ε in the left panel. Again, the decrease in the peak height of SNR due to increasing ε is obvious, but in addition, the spreading of the enhanced correlation with the localized periodic driving to units far from the pacemaker-driven oscillator is evident as well. The inset in figure 4 features a color map evidencing the decay of peak SNR values and the accompanying spreading to more and more distinct units as ε increases, thus additionally supporting conclusions derived from the two main graphs.

We argue that the noise-supported spreading of the outreach of a localized subthreshold periodic driving in a diffusively coupled network of bistable oscillators can be explained by the classic law of diffusion in that, while the peak value of SNR decays proportionally to $\varepsilon^{-1/2}$, the area under the SNR curve in dependence on i is preserved. Indeed, the area under different curves in the right panel of figure 4 is equal for all ε within $\pm 3\%$, and the drop of the maximal SNR is rather accurately proportional to $\varepsilon^{-1/2}$ as shown in figure 5. The outlined compliance of the SNR dependence on i with the diffusive law is, however, not particularly startling because the underlying network of the model dictates precisely such a spreading of localized perturbations. While this spreading may be optimized by an appropriate amount of additive Gaussian noise as evidenced earlier, there is no reason why the diffusive law would be violated. Different observations will be made in the next two sections, where the topology of the underlying network, being either of small-world or scale-free type, clearly violates the basic premise of diffusive spreading, either due to the introduction of shortcut links between distinct

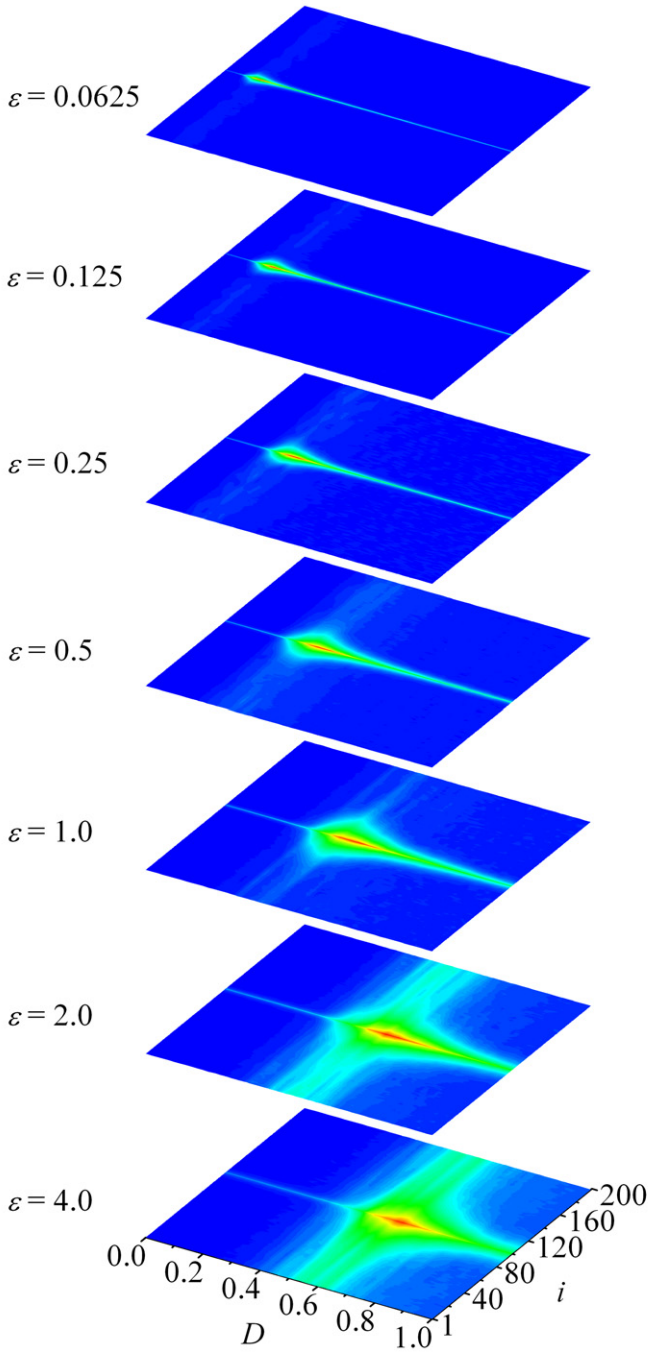

Figure 3. Color-coded SNR in dependence on D and i for different ε, obtained when the diffusive networks are governed by the bistable dynamics. In all panels, the pacemaker has been introduced to the middle oscillator $i = r = 100$ and the color profile is linear, blue marking minimal and red maximal values of SNR. The specific intervals of SNR from top to bottom are: 0.0–0.2, 0.0–0.14, 0.0–0.093, 0.0–0.066, 0.0–0.045, 0.0–0.032 and 0.0–0.024 (note that the overall maximum of SNR decreases continuously as ε increases).

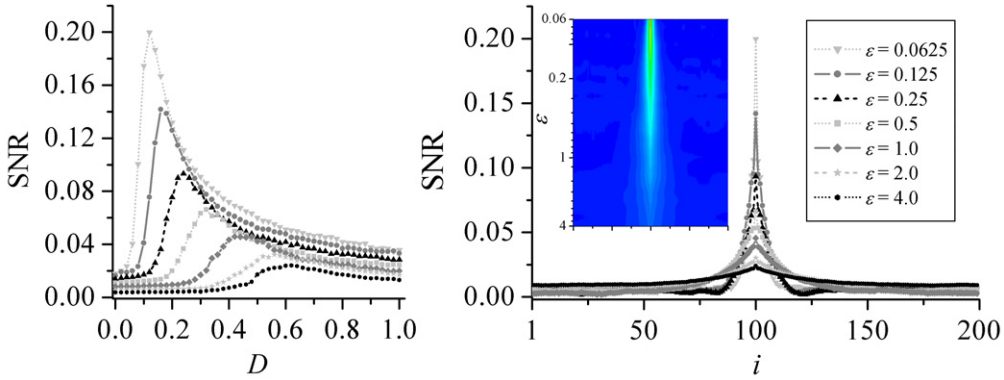

Figure 4. Characteristic cross-sections of color maps presented in figure 3. Left panel: SNR in dependence on D for the oscillator $i = r = 100$ that is under the direct influence of the pacemaker. Right panel: SNR in dependence on i by the value of D warranting the peak SNR by a given ε in the left panel. The inset additionally features the same SNR color-coded, blue marking minimal (0.0) and red maximal values (0.2), in dependence on i and ε.

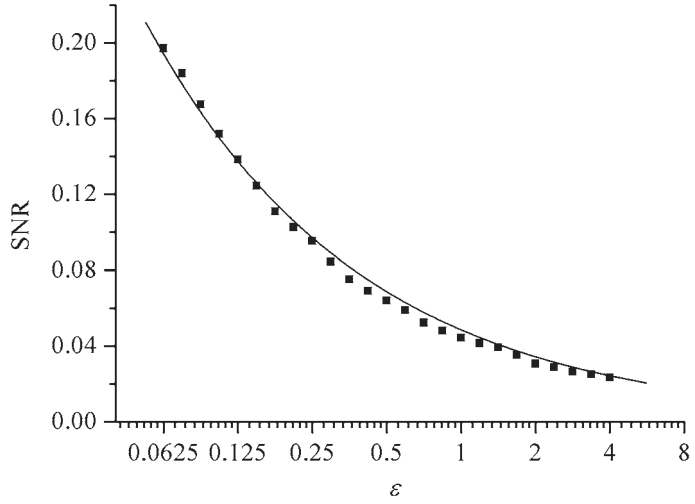

Figure 5. Decay of the overall peak height of SNR in dependence on ε for $p = 0.0$, obtained when the diffusive network is governed by the bistable dynamics. Squares are numerically obtained values, whereas the line represents a fit via $w\varepsilon^{-1/2}$, w being a numerically determined constant presently equaling 0.048.

units of the network [16] as exemplified in figure 1(b), or due to the highly inhomogeneous degree distribution resulting from growth and preferential attachment [17].

4. Small-world networks

In this section, we present the results obtained if the diffusive coupling of bistable oscillators is relaxed via the introduction of a certain fraction p of shortcuts amongst arbitrary units of the

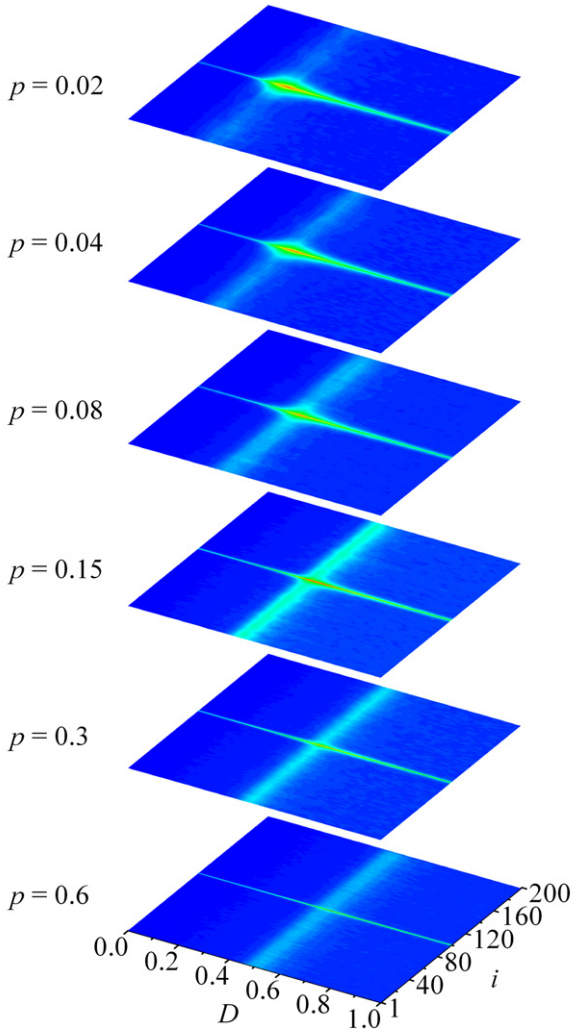

Figure 6. Color-coded SNR in dependence on D and i for different p, obtained if the small-world networks are governed by the bistable dynamics. In all panels the pacemaker has been introduced to the middle oscillator $i = r = 100$ and the color profile is linear, blue marking minimal and red maximal values of SNR. The specific intervals of SNR from top to bottom are: 0.0–0.059, 0.0–0.053, 0.0–0.048, 0.0–0.04, 0.0–0.037 and 0.0–0.033 (note that the overall maximum of SNR decreases continuously as p increases).

network. First, we set $\varepsilon = 0.5$ and examine the dependence of SNR on D and i for different p. Figure 6 features the resulting color-contour plots for increasing values of p from top to the bottom panel. As for the diffusive coupling, it is evident that there exists an optimal D by which the SNR is maximal. Although the stochastic resonance phenomenon is better expressed for units that are in the immediate proximity of the oscillator $i = r = 100$ that is under the direct influence of the pacemaker, the fine-tuning of p clearly has the ability to optimally facilitate the outreach of the localized subthreshold periodic forcing. In particular, for $p = 0.15$ *all* units of the network feature the best expressed bell-shaped dependence of the SNR on D, whereas for smaller and larger p this feature deteriorates substantially. Hence, results presented in figure 6

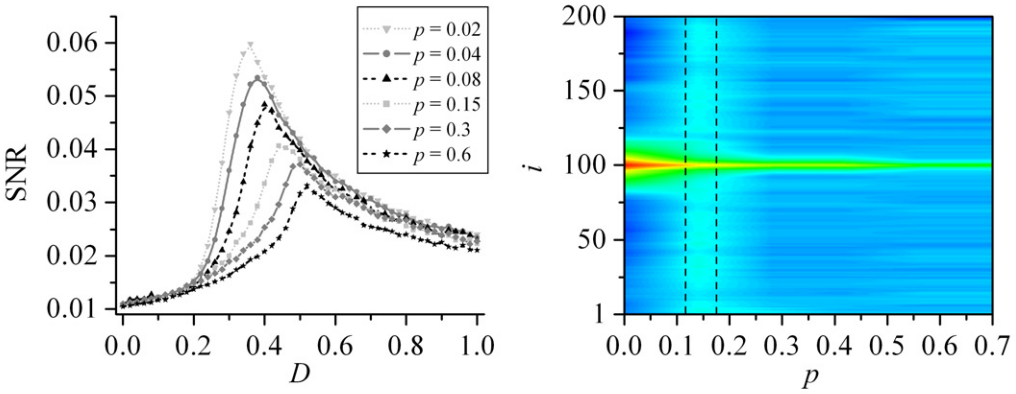

Figure 7. Characteristic cross-sections of color maps presented in figure 6. Left panel: SNR in dependence on D for the oscillator $i = r = 100$ that is under the direct influence of the pacemaker. Right panel: color-coded SNR in dependence on p and i by the value of D warranting the peak SNR for a given p in the left panel. The color profile is logarithmic, blue marking SNR $= 0.005$ and red SNR $= 0.066$.

indicate that there exists an optimal small-world topology for the transmission of localized rhythmic activity across a noisy array of bistable oscillators.

To study the above possibility more precisely, and to give a better quantitative view of the results presented in figure 6, we examine characteristic cross-sections of the examined color maps. The left panel of figure 7 features SNR curves in dependence on D only for the oscillator that is under the direct influence of the pacemaker. As for the diffusive coupling, this is the unit of the network by which the most correlated response with respect to the subthreshold periodic driving sets in, and accordingly, the overall maximal SNR is obtained. Results in the left panel of figure 7 have a remarkable qualitative resemblance with those presented in the left panel of figure 4. Likewise as in figure 4 due to increasing values of ε, in figure 7 the optimal D increases continuously (and accordingly the peak value of SNR decays) as p increases. It thus may be argued that the introduction of shortcut links acts similarly, at least on the unit that is directly perturbed by the pacemaker, as the increase of coupling strength. Indeed, this is easy to justify as shortcuts effectively shorten the distance between units, and thus a localized stimulus is able to reach a distant unit faster. While larger ε of course do not shorten the distance between units, they do, however, increase the speed (the rate of diffusive spread) at which a locally emitted perturbation travels to other units, which in turn results in a faster transfer, similarly, as if the effective path were shortened. Turning back to establishing the existence of an optimal p, results in the left panel of figure 7 allow us to determine the optimal D in dependence on p. We use these values to examine the cross-sections of colored maps in figure 6 along i. The right panel of figure 7 features a colored map depicting SNR values in dependence on p and i for the value of D giving the peak SNR for a given p in the left panel. Again, the decrease in the peak height of SNR due to increasing p is obvious, but in addition, the optimal spreading of the enhanced correlation with the localized periodic driving to units far from the pacemaker-driven oscillator occurring for $p \approx 0.15$ is clearly evident as well (marked additionally by two dashed vertical lines). We thus conclude that there exists an optimal small-world topology for the transmission of localized rhythmic activity across a noisy array of bistable oscillators.

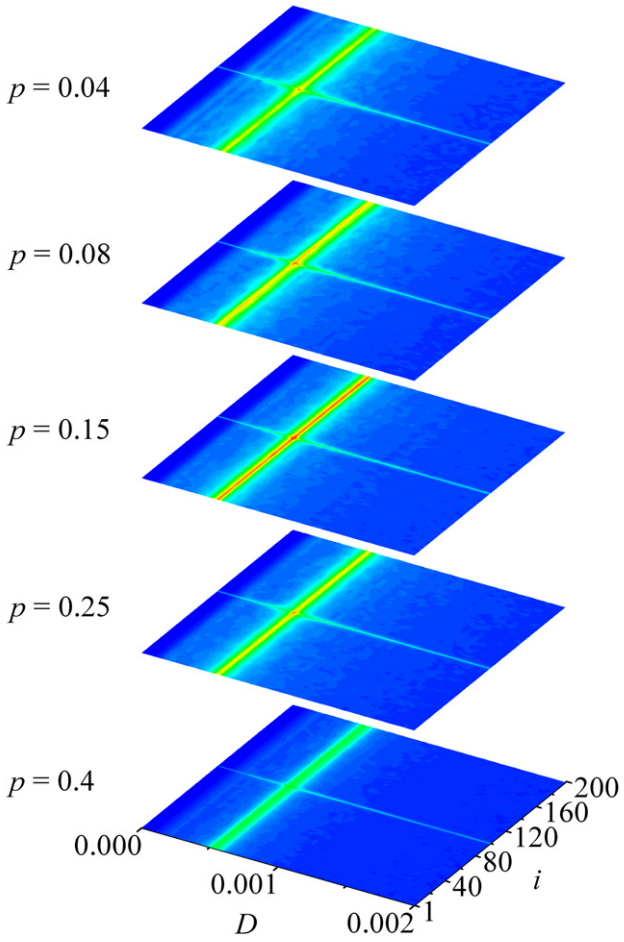

Figure 8. Color-coded SNR in dependence on D and i for different ε, obtained when the small-world networks are governed by the FitzHugh–Nagumo excitable dynamics [equation (2)]. In all panels the pacemaker has been introduced to the middle oscillator $i = r = 100$ and the color profile is linear, blue marking minimal (0.0) and red maximal (0.03) values of SNR.

In order to further strengthen the existence of the optimal p and to widen the scope of this finding, we substitute the bistable model considered so far with the FitzHugh–Nagumo excitable dynamics described by equation (2). We set $\varepsilon = 0.2$, and as in figure 6, examine the dependence of SNR on D and i for different p. Results are presented in figure 8 for increasing values of p from the top to the bottom panel. As for the bistable dynamics, there always exists an optimal D by which the SNR is maximal, and moreover, for small p the stochastic resonance is better expressed for units that are in the immediate proximity of the unit $i = r = 100$ that is under the direct influence of the pacemaker. However, as p increases, we can again observe the existence of an optimal topology for which the outreach of the localized subthreshold periodic forcing optimally extends across all coupled units. In particular, for $p = 0.15$ peak SNR values remain large, yet are almost equally distributed across all units. Smaller p localize the optimal response to units within the proximity of $i = r = 100$, whereas larger p induce an overall decrease of peak SNR values. Thus, even if the bistable overdamped oscillator is replaced by the excitable

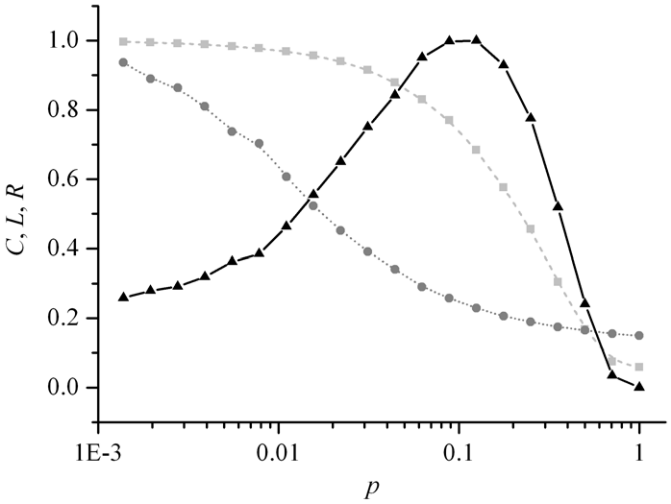

Figure 9. Normalized clustering coefficient C (squares), normalized characteristic path length L (circles), and the ratio $R = C/L$ (triangles) in dependence on p for a network consisting of $N = 200$ vertices having average connectivity $k = 4$. Results were averaged over 50 different realizations of each network, and the ratio R was uniformly rescaled to the unit interval (the shape of the dependence on p was completely preserved) for better comparisons of all three curves. Lines are solely a guide to the eye.

FitzHugh–Nagumo system, the optimal small-world topology warranting the best transmission of localized rhythmic activity prevails.

Aiming to explain the existence of the above-established optimal small-world topology, we employ classical measures such as the normalized characteristic path length L and the normalized clustering coefficient C [16], as defined in section 2. While L is often the more appraised quantity (echoing in the name 'small-world' describing such networks), the clustering coefficient is presently also crucial since it quantifies to what extent local interactions are intact or broken. In particular, $C = 1$ means that the cliquishness of the nearest neighbors is perfect, whereas $C = 0$ means that the neighbors connected to a given unit of the network are disconnected from one another. Since the effectiveness of the pacemaker to transmit its rhythm also to units that are not within its immediate proximity relies both on effective nearest-neighbor interactions as well as on the ability to reach physically distant units to which excitations might die out via the diffusive route, we propose the ratio between the normalized clustering coefficient and the characteristic path length $R = C/L$ as the crucial quantity defining the optimal properties of a network to facilitate the spreading of a localized pacemaker-emitted rhythmic activity. The higher the value of R, the better the network structure is adapted to enforce the pacemaker activity on other network units. A high value of R suggests that the nearest-neighbor interactions are largely intact, while at the same time considerable benefits in terms of excitation propagation may be expected from long-range connections. On the other hand, a low value of R indicates either that nearest-neighbor interactions are largely broken or that long-range connections are sparse, whereby any of these two properties would act detrimentally on the ability of a pacemaker to enforce its rhythm on other units of the network. Results for the presently employed network ($N = 200$, $k = 4$) are shown in figure 9.

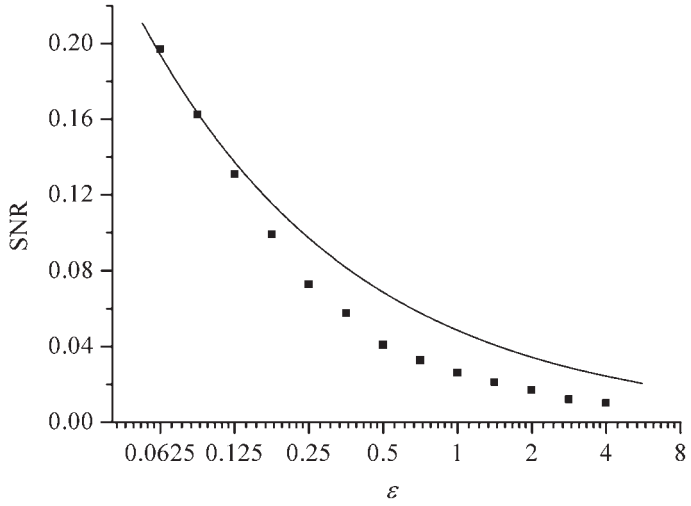

Figure 10. Decay of the overall peak height of SNR in dependence on ε for $p = 0.15$, obtained when the small-world network is governed by the bistable dynamics. Squares are numerically obtained values, whereas the line shows the same $w\varepsilon^{-1/2}$ fit as depicted in figure 5. The decay is clearly faster than on a diffusive network due to the introduction of small-world connectivity.

Indeed, the peak value of R is obtained by roughly the same value of the small-world connectivity, equaling $p \approx 0.15$, that also warrants the best outreach of the pacemaker to units that are not in its immediate proximity. This result confirms our reasoning and introduces a compact measure for assessing the ability of a small-world network topology to promote the spreading of localized rhythmic activity across coupled units.

It is noteworthy that, by comparing the results presented in figures 4 and 7 obtained for the bistable dynamics, it becomes obvious that while the effect of increasing ε and p is similar with respect to the continuous decrease of the overall maximal SNR observed by the pacemaker-driven unit, it is in fact qualitatively different with respect to warranting the best possible outreach of the pacemaker to units that are not within its immediate proximity in the network. In particular, while increasing values of ε continuously improves the outreach of the pacemaker (albeit at the expense of the decaying correlation with the pacemaker-driven unit), increasing values of p start destroying it once an optimal value, presently equaling $p \approx 0.15$, is exceeded. It thus seems appropriate to examine whether the introduction of small-world connectivity introduces qualitatively new behavior with respect to ε as well, which might in turn explain the facilitation of the pacemaker's outreach by the optimal p. To study this, we set $p = 0.15$ and examine how the overall peak of SNR (obtained by scanning the parameter space over D and i) decays in dependence on ε if the bistable model is considered. Results presented in figure 10 show that, indeed, the decay and with it related outreach of the pacemaker to distant units, no longer obey the classic law of diffusion exemplified in figure 5. In fact, the decay is faster, clearly departing from the $\varepsilon^{-1/2}$ dependence especially towards larger ε. This result indicates that on a small-world network the outreach of the pacemaker is no longer governed by the classic diffusion but becomes superdiffusive, which in turn additionally explains the increase of its range and effectiveness for an appropriate value of p.

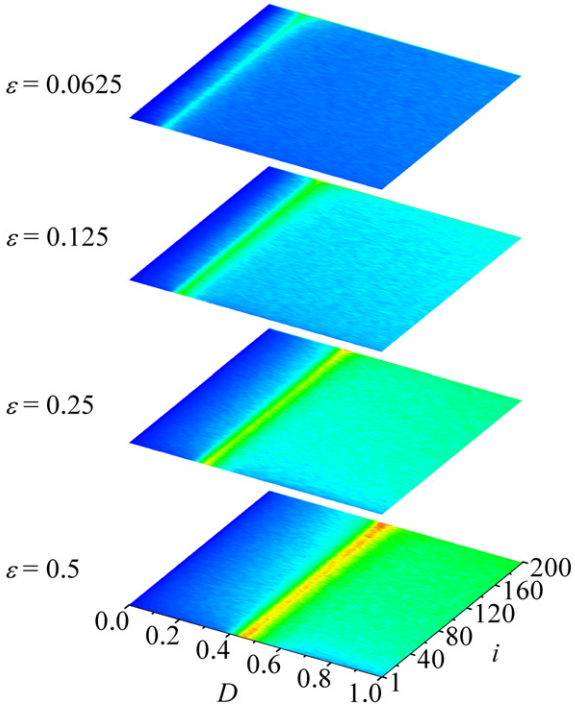

Figure 11. Color-coded SNR in dependence on D and i for different ε, obtained when the scale-free networks are governed by the bistable dynamics. In all panels the pacemaker has been introduced to the main hub of the scale-free network $i = r = 200$ and the color profile is linear, blue marking minimal and red maximal values of SNR. The specific intervals of SNR from top to bottom are: 0.0–0.046, 0.0–0.025, 0.0–0.016 and 0.0–0.013 (note that the overall maximum of SNR decreases continuously as ε increases).

5. Scale-free networks

Finally, it remains of interest to examine results obtained if the underlying interaction topology of bistable overdamped oscillators is of scale-free type. Figure 11 features color-contour plots of SNR in dependence on D and i for different ε. As for previously considered networks, there exists an optimal value of D for which the response of units is optimally correlated with the frequency of the pacemaker, thus evidencing pacemaker-driven stochastic resonance on scale-free networks of bistable oscillators. Remarkably, irrespective of ε the outreach of the pacemaker extends nearly equally across all units, especially if compared with results obtained for diffusive networks presented in figure 3. Moreover, by considering the bottom panel of figure 11 featuring results obtained by $\varepsilon = 0.5$ and comparing it with the panel showing results for $p = 0.15$ in figure 6 for the same ε, it can be concluded that the scale-free topology warrants the best noise-supported dissemination of pacemaker-emitted rhythmic activity across *the whole* network. Nevertheless, the correlation between the pacemaker and the unit (main hub) that is under its direct influence (having index $i = r = 200$ in figure 11) is smaller than that for the two previously considered network types.

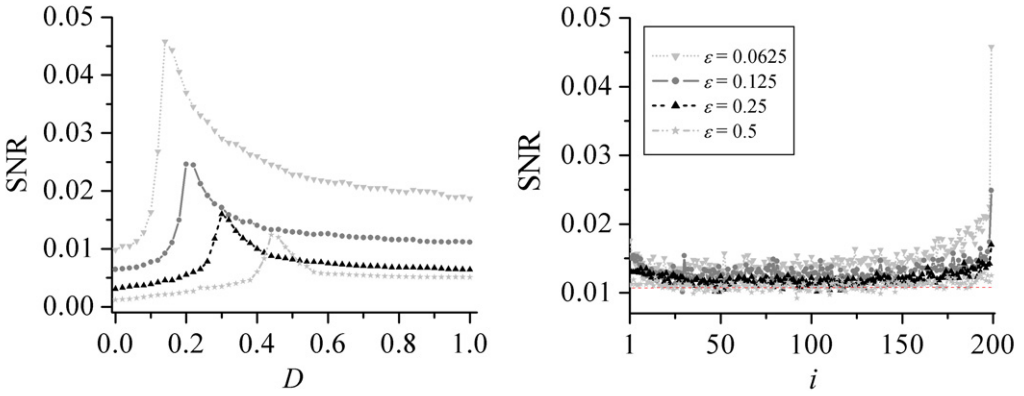

Figure 12. Characteristic cross-sections of color maps presented in figure 11. Left panel: SNR in dependence on D for the unit (main hub of the network) $i = r = 200$ that is under the direct influence of the pacemaker. Right panel: SNR in dependence on i for the value of D giving the peak SNR for a given ε in the left panel.

To give a better quantitative view of these claims, we examine characteristic cross-sections of colored maps presented in figure 11. The left panel of figure 12 features SNR curves in dependence on D for the oscillator $i = r = 200$ that is under the direct influence of the pacemaker. It is evident that, similarly as shown in the left panel of figure 4, the peak value of SNR decreases and moves toward higher D as ε increases. As for the diffusive and small-world coupling, the paced oscillator $i = r = 200$ should be the unit of the network by which the most correlated response with respect to the subthreshold periodic driving sets in, resulting in the overall peak SNR for each particular ε. However, by simultaneously considering also the results presented in the right panel of figure 12, it becomes quickly obvious that for $\varepsilon \geqslant 0.25$ the SNR for the optimal D (derived from the left panel) is, aside from small-amplitude deviations, practically equal for all units i. This fact is additionally put forward by a dashed red line depicted in the right panel of figure 12, indicating the plateau for $\varepsilon = 0.5$. Only for $\varepsilon = 0.125$, and even more so for $\varepsilon = 0.0625$, the peak SNR for the paced main hub ($i = r = 200$) is substantially larger than that for other constitutive units of the scale-free network. Nevertheless, by reaching 0.046 if $\varepsilon = 0.0625$, the overall peak SNR is still more than five times smaller than under the same conditions on a diffusive network (see inverted triangles in figure 4), which is the cost of an effective transmission of the pacemaker rhythm across all units. We argue that the scale-free topology enables the latter due to its distinct inhomogeneous property [17] via which individual units, and particularly the main hub, have the ability to instantly and directly influence many other constitutive units of the network, and thus effectively (superdiffusively) propagate the pacemaker-emitted rhythmic activity.

To generalize our findings related to the scale-free network topology, we again substitute the bistable model with the FitzHugh–Nagumo excitable dynamics and repeat the calculations for $\varepsilon = 0.2$. Note that the same coupling strength has already been considered in figure 8 when examining the noise-induced dynamics on small-world networks. The left panel of figure 13 features the obtained color-contour plot of SNR in dependence on D and i. The presented results are truly convincing, as it is completely impossible to infer the index i of the main hub hosting

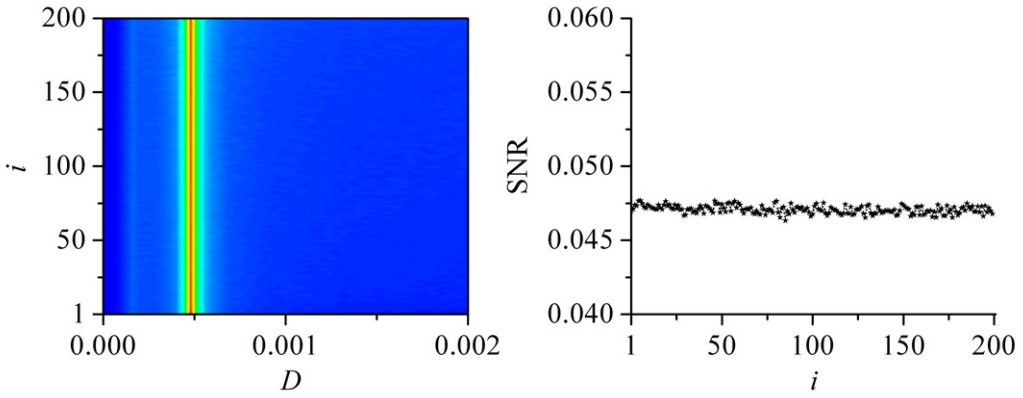

Figure 13. Left panel features color-coded SNR in dependence on D and i for $\varepsilon = 0.5$, obtained when the scale-free network is governed by the FitzHugh–Nagumo excitable dynamics. The pacemaker has been introduced to the main hub of the scale-free network $i = r = 200$ and the color profile is linear, blue marking minimal (0.0) and red maximal (0.048) values of SNR. The right panel shows the cross-section of the color map across all i obtained for $D = 0.00048$.

the pacemaker (it is $i = r = 200$ as in figure 11). In other words, all units of the network are equally well correlated with the frequency of the pacemaker, which is additionally emphasized in the right panel of figure 13 featuring the cross-section of the left panel for the optimal D. Thus, irrespective of whether the network dynamics is bistable or excitable, the scale-free topology warrants the best noise-supported dissemination of locally imposed rhythmic activity across the whole network, outperforming the diffusive as well as the small-world topology.

6. Summary

There exists several natural and artificial bistable signaling devices that are connected via networks. Presently, we employ different networks of overdamped bistable oscillators to study the phenomenon of stochastic resonance brought about by a subthreshold pacemaker. We introduce the pacemaker in the form of a subthreshold periodic forcing to a single oscillator of the network. With the aid of additive Gaussian noise, the pacemaker tries to enforce its rhythm on the whole network, and hence we observe an interesting interplay between noise, coupling strength, network topology and the outreach of the pacemaker. First, we examine only nearest-neighbor interactions among coupled units. We show that the response of the pacemaker-driven unit and the network as a whole is resonantly dependent on the noise intensity, as only an appropriate intensity of additive noise ensures the optimal correlation between the pacemaker signal and jumps between the stable steady states of overdamped oscillators. However, the outreach of the pacemaker decays with the distance from its origin rather fast. We investigate this phenomenon thoroughly, and show that the impact of the pacemaker on other units is proportional to the square root of the coupling strength, thus obeying the classical law of diffusion. Second, we introduce the small-world topology among coupled oscillators, where our results indicate that for a suitable fraction of rewired links the spreading of pacemaker activity is pronounced best. Namely, due to the introduction of shortcut links, the

effective distance between units shortens, and accordingly, the localized stimulus is able to reach distant units faster without the accompanying loss of strength occurring by diffusive coupling. Moreover, if at the same time the clustering coefficient of the small-world network is comparable with that of a diffusive network, the nearest-neighbor connections responsible for an effective impact by units in the immediate vicinity of the pacemaker are also largely preserved, which combined yields an optimal topology for the spreading of localized rhythmic activity across all coupled units. We additionally support these arguments by considering, as an alternative to the bistable dynamics, the excitable FitzHugh–Nagumo system, in particular, by showing that the qualitative change in the properties of the governing differential equations does not induce different results. In addition, our calculations indicate that by the optimal small-world topology the outreach of the subthreshold periodic forcing is no longer diffusive but becomes superdiffusive, thus providing an explanation for the small-world-related facilitation of the pacemaker's influence on the whole network. Finally, we examine the effects of scale-free network topology on the phenomenon of pacemaker-driven stochastic resonance, and find that it is optimal for the transmission of weak localized rhythmic activity across the whole network. This is attributed to the distinct inhomogeneous structure of scale-free networks via which individual units (hubs) have the ability to instantly influence many other units, and thus effectively propagate the pacemaker-induced rhythm. As for the small-world topology, these network-related features are shown to apply irrespective of the particularities of the governing dynamics. Due to the significant importance of pacemakers in various networks connecting natural and artificial systems, we hope our study will be applicable in real-life motivated problems, and foster the understanding of processes whose proper functioning relies on an effective pacemaker.

Acknowledgment

Matjaž Perc acknowledges support from the Slovenian Research Agency (grant Z1-9629).

References

[1] Horsthemke W and Lefever R 1984 *Noise-Induced Transitions* (Berlin: Springer)
Hänggi P and Bartussek R 1999 *Nonlinear Physics of Complex Systems* ed J Parisi, S C Müller and W Zimmermman (New York: Springer)
[2] Jung P 1993 *Phys. Rep.* **234** 175
Moss F, Bulsara A and Shlesinger M F 1993 *J. Stat. Phys.* **70** 1
Gammaitoni L, Hänggi P, Jung P and Marchesoni F 1998 *Rev. Mod. Phys.* **70** 223
[3] Sigeti D and Horsthemke W 1989 *J. Stat. Phys.* **54** 1217
Hu G, Ditzinger T, Ning C Z and Haken H 1993 *Phys. Rev. Lett.* **71** 807
Rappel W J and Strogatz S H 1994 *Phys. Rev.* E **50** 3249
Pikovsky A S and Kurths J 1997 *Phys. Rev. Lett.* **78** 775
Longtin A 1997 *Phys. Rev.* E **55** 868
[4] Benzi R, Sutera A and Vulpiani A 1981 *J. Phys. A: Math. Gen.* **14** L453
Nicolis C and Nicolis G 1981 *Tellus* **33** 225
Gammaitoni L, Marchesoni F, Menichella-Saetta E and Santucci S 1989 *Phys. Rev. Lett.* **62** 349
Jung P and Hänggi P 1991 *Phys. Rev.* A **44** 8032

[5] Longtin A 1993 *J. Stat. Phys.* **70** 309
[6] Pradines J R, Osipov G V and Collins J J 1999 *Phys. Rev.* E **60** 6407
Ullner U, Zaikin A A, Garcia-Ojavo J, Báscones R and Kurths J 2003 *Phys. Lett.* A **312** 348
Volkov E I, Ullner U, Zaikin A A and Kurths J 2003 *Phys. Rev.* E **68** 026214
Tessone C J, Ullner E, Zaikin A A, Kurths J and Toral R 2006 *Phys. Rev.* E **74** 046220
Perc M and Szolnoki A 2007 *New J. Phys.* **9** 267
Lindner B, García-Ojalvo J, Neiman A and Schimansky-Geier L 2004 *Phys. Rep.* **392** 321
[7] Neiman A, Saparin P I and Stone L 1997 *Phys. Rev.* E **56** 270
Hou Z and Xin H 1999 *Phys. Rev.* E **60** 6329
Rozenfeld A, Tessone C J, Albano E and Wio H S 2001 *Phys. Lett.* A **280** 45
Katsev S and L'Heureux I 2000 *Phys. Rev.* E **61** 4972
Ushakov O V, Wünsche H-J, Henneberger F, Khovanov I A, Schimansky-Geier L and Zaks M A 2005 *Phys. Rev. Lett.* **95** 123903
Sethia G C, Kurths J and Sen A 2007 *Phys. Lett.* A **364** 227
Xiao T, Ma J, Hou Z and Xin H 2007 *New J. Phys.* **9** 403
[8] Nicolis G, Nicolis C and McKernan D 1993 *J. Stat. Phys.* **70** 125
Palenzuela C, Toral R, Mirasso C R, Calvo O and Gunton J D 2001 *Europhys. Lett.* **56** 347
[9] Jung P, Behn U, Pantazelou E and Moss F 1992 *Phys. Rev.* A **46** R1709
Bulsara A R and Schmera G 1993 *Phys. Rev.* E **47** 3734
Gang H, Haken H and Fagen X 1996 *Phys. Rev. Lett.* **77** 1925
[10] Lindner J F, Meadows B K, Ditto W L, Inchiosa M E and Bulsara A R 1995 *Phys. Rev. Lett.* **75** 3
Löcher M, Johnson G A and Hunt E R 1996 *Phys. Rev. Lett.* **77** 4698
Lindner J F, Meadows B K, Ditto W L, Inchiosa M E and Bulsara A R 1996 *Phys. Rev.* E **53** 2081
Sungar N, Sharpe J P and Weber S 2000 *Phys. Rev.* E **62** 1413
[11] Tessone C J, Mirasso C R, Toral R and Gunton J D 2006 *Phys. Rev. Lett.* **97** 194101
[12] Pikovsky A, Zaikin A and de la Casa M A 2002 *Phys. Rev. Lett.* **88** 050601
[13] Jung P and Mayer-Kress G 1995 *Phys. Rev. Lett.* **74** 2130
[14] García-Ojalvo J and Sancho J M 1999 *Noise in Spatially Extended Systems* (New York: Springer)
Wang J 2001 *Chem. Phys. Lett.* **339** 357
Busch H and Kaiser F 2003 *Phys. Rev.* E **67** 041105
Ullner E, Zaikin A A, García-Ojalvo J and Kurths J 2003 *Phys. Rev. Lett.* **91** 180601
Carrillo O, Santos M A, García-Ojalvo J and Sancho J M 2004 *Europhys. Lett.* **65** 452
Roussel M R and Wang J 2004 *J. Chem. Phys.* **120** 8079
Zhou C S and Kurths J 2005 *New J. Phys.* **7** 18
Glatt E, Busch H, Kaiser F and Zaikin A 2006 *Phys. Rev.* E **73** 026216
Wang Q Y, Lu Q S and Chen G R 2007 *Europhys. Lett.* **77** 10004
Perc M, Gosak M and Marhl M 2007 *Chem. Phys. Lett.* **437** 143
Gosak M, Marhl M and Perc M 2007 *Biophys. Chem.* **128** 210
Nekhamkina O and Sheintuch M 2007 *Phys. Rev.* E **75** 056210
Wang Q Y, Duan Z S, Huang L, Chen G R and Lu Q S 2007 *New J. Phys.* **9** 383
Sagués F, Sancho J M and García-Ojalvo J 2007 *Rev. Mod. Phys.* **79** 829
[15] Albert R and Barabási A-L 2002 *Rev. Mod. Phys.* **74** 47
Boccaletti S, Latora V, Moreno Y, Chavez M and Hwang D-U 2006 *Phys. Rep.* **424** 175
[16] Watts D J and Strogatz S H 1998 *Nature* **393** 440
[17] Barabási A-L and Albert R 1999 *Science* **286** 509
[18] Wasserman S and Faust K 1994 *Social Network Analysis* (Cambridge: Cambridge University Press)
[19] Van Raan A F J 1990 *Nature* **347** 626
Seglen P O 1992 *J. Am. Soc. Inf. Sci.* **43** 628
Redner S 1998 *Eur. Phys. J.* B **4** 131

[20] McCann K, Hastings A and Huxel G R 1998 *Nature* **395** 794
Hart D R, Berman T and Stone L 2000 *Limnol. Oceanogr.* **45** 350
Berlow E L *et al* 2004 *J. Anim. Ecol.* **73** 585
Quince C, Higgs P G and McKane A J 2005 *Ecol. Model.* **187** 389
Srinivasan U T, Dunne J A, Harte J and Martinez N D 2007 *Ecology* **88** 671
Fussmann G F 2007 *Complex Population Dynamics* ed B Blasius, J Kurths and L Stone *Lecture Notes in Complex Systems* vol 7 (Singapore: World Scientific)
[21] Huberman B A and Adamic L A 1999 *Nature* **401** 131
Adamic L A, Huberman B A, Barabási A-L, Albert R, Jeong H and Bianconi G 2000 *Science* **287** 2115
[22] Lago-Fernández L F, Huerta R, Corbacho F and Sigüenza J A 2000 *Phys. Rev. Lett.* **84** 2758
Shefi O, Golding I, Segev R, Ben-Jacob E and Ayali A 2002 *Phys. Rev.* E **66** 021905
Roxin A, Riecke H and Solla S A 2004 *Phys. Rev. Lett.* **92** 198101
Eguíluz V M, Chialvo D R, Gecchi G, Baliki M and Apkarian A V 2005 *Phys. Rev. Lett.* **94** 018102
Volman V, Baruchi I and Ben-Jacob E 2005 *Phys. Biol.* **2** 98
Swain P K and Longtin A 2006 *Chaos* **16** 026101
Masuda N, Okada M and Aihara K 2007 *Neural Comput.* **19** 1854
[23] Gao Z, Hu B and Hu G 2001 *Phys. Rev.* E **65** 016209
Hong H, Kim B J and Choi M Y 2002 *Phys. Rev.* E **66** 011107
[24] Kuperman M and Zanette D 2002 *Eur. Phys. J.* B **26** 387
[25] Acebrón J A, Lozano S and Arenas A 2007 *Phys. Rev. Lett.* **99** 128701
[26] Kwon O and Moon H-T 2002 *Phys. Lett.* A **298** 319
Kwon O, Jo H-H and Moon H-T 2005 *Phys. Rev.* E **72** 066121
[27] He D, Hu G, Zhan M, Ren W and Gao Z 2002 *Phys. Rev.* E **65** 055204
Wang X, Lu Y, Jiang M and Ouyang Q 2004 *Phys. Rev.* E **69** 056223
Perc M 2005 *New J. Phys.* **7** 252
[28] Gong Y, Xu B, Xu Q, Yang C, Ren T, Hou Z and Xin H 2006 *Phys. Rev.* E **73** 046137
Wie D Q and Luo X S 2007 *Europhys. Lett.* **78** 68004
[29] Nagai Y, González H, Shrier A and Glass L 2000 *Phys. Rev. Lett.* **84** 4248
Alonso S, Sendiña-Nadal I, Pérez-Muñuzuri V, Sancho J M and Sagués F 2001 *Phys. Rev. Lett.* **87** 078302
Gutman M, Aviram I and Rabinovitch A 2004 *Phys. Rev.* E **70** 037202
Smolka L B, Marts B and Lin A L 2005 *Phys. Rev.* E **72** 056205
Jacquemet V 2006 *Phys. Rev.* E **74** 011908
Perc M and Marhl M 2006 *Phys. Lett.* A **353** 372
Chigwada T R, Parmananda P and Showalter K 2006 *Phys. Rev. Lett.* **96** 244101
[30] Kori H and Mikhailov A S 2004 *Phys. Rev. Lett.* **93** 254101
Radicchi F and Meyer-Ortmanns H 2006 *Phys. Rev.* E **73** 036218
Steele A J, Tinsley M and Showalter K 2006 *Chaos* **16** 015110
[31] Fitzhugh R 1961 *Biophys. J.* **1** 445
Nagumo J S, Arimoto S and Yoshizawa S 1962 *Proc. IRE* **50** 2061
[32] Desai R C and Zwanzig R 1978 *J. Stat. Phys.* **19** 1
[33] Press W H, Teukolsky S A, Vetterling W T and Flannery B P 1995 *Numerical Recipes in C* (Cambridge: Cambridge University Press)
[34] Holden L and Erneux Z 1993 *SIAM J. Appl. Math.* **53** 1045